Effects of scattering centers on the energy spectrum of a quantum dot

V. Halonen, P. Hyvönen, and P. Pietiläinen
Theoretical Physics, University of Oulu, FIN-90570 Oulu, Finland

Tapash Chakraborty
Institute of Mathematical Sciences, Taramani, Madras 600 113, India

(Received 16 October 1995)

Repulsive scattering centers in quantum dots have profound effects on the energy spectrum of a quantum dot in a magnetic field. The symmetry-breaking electron-impurity potentials cause lifting of the degeneracy, level repulsion, etc. in the energy spectrum and angular momentum selection rules are found that govern those anticrossings of the energy levels. We also study the optical absorption spectra in the presence of single or multiple scatterers in a parabolic dot.

Quantum-confined few-electron systems, or quantum dots, have received increasing attention in recent years because of the many interesting physical properties observed in these systems[1–4] as well as potentials for future technological applications.[5] While most of the theoretical work so far have been confined to electronic states in impurity-free systems, here we report our work on the effect of repulsive scattering centers on the energy spectrum of a quantum dot in a magnetic field. The breaking of circular symmetry due to the impurity potential introduces a lot of additional structures due to level repulsions, lifting of degeneracy, etc. in the otherwise well understood spectrum of an impurity-free parabolic quantum dot.[1] We have analyzed those structures and extracted some simple rules when the level repulsions are found to occur. We should point out that transport properties of quantum dots with an impurity that can be controlled independently are under active investigations[6] and energy spectra like the ones presented here can be observed in experiments like single-electron capacitance spectroscopy and optical spectroscopy.[4]

We have used the standard model[1] in which electrons of effective mass m^* are confined within the $z=0$ plane by a parabolic potential and are subjected to a perpendicular magnetic field B. In the presence of a symmetry-breaking impurity potential, the many-electron Hamiltonian is written as

$$\mathscr{H}=\frac{1}{2m^*}\sum_{i=1}^{n_e}\left(\mathbf{p}_i+\frac{e}{c}\mathbf{A}_i\right)^2+\frac{1}{2}m^*\omega_0^2\sum_{i=1}^{n_e}r_i^2+\sum_{i=1}^{n_e}V^{\mathrm{imp}}(\mathbf{r}_i)+\frac{1}{2}\frac{e^2}{\epsilon}\sum_{i\neq j}\frac{1}{|\mathbf{r}_i-\mathbf{r}_j|}, \tag{1}$$

where n_e is the number of electrons in the system and ϵ is the background dielectric constant. We also use the symmetric gauge vector potential, $\mathbf{A}=\frac{1}{2}(-By,Bx,0)$. The impurities are modeled by a Gaussian potential

$$V^{\mathrm{imp}}(\mathbf{r})=V_0e^{-(\mathbf{r}-\mathbf{R})^2/d^2}, \tag{2}$$

where V_0 is the potential strength, d is proportional to the width of the impurity potential (the full width at half maximum $\approx 1.67d$), and $\mathbf{R}$ is the position of the impurity. We apply the exact diagonalization method by constructing the basis using the single-particle wave functions of a perfect parabolic quantum dot[3]

$$\varphi_{\mathrm{nl}}(\mathbf{r})=Ce^{-il\theta-r^2/(2a^2)}r^{|l|}L_n^{|l|}(r^2/a^2), \tag{3}$$

where C is the normalization constant, $a=\sqrt{\hbar/(m^*\Omega)}$, $\Omega=\sqrt{\omega_0^2+\omega_c^2/4}$, and $L_n^k(x)$ is the associated Laguerre polynomial. The quantum number $l=0,\pm1,\pm2,\ldots$ is the orbital angular momentum quantum number and $n=0,1,2,\ldots$ is the radial quantum number. In the actual calculations electron spins are taken into account but the Zeeman energy is ignored.

The impurity potential $V^{\mathrm{imp}}(\mathbf{r})$ introduces an interaction between the single-particle states $\varphi_{\mathrm{nl}}(\mathbf{r})$ with matrix elements

$$\begin{aligned}\int\varphi^*_{n_1l_1}(\mathbf{r})V^{\mathrm{imp}}(\mathbf{r})\varphi_{n_2l_2}(\mathbf{r})d\mathbf{r}&=V_0e^{-i(l_1-l_2)\Theta}(d/a)^2(R/a)^ke^{-(R/a)^2/[1+(d/a)^2]}\\&\times\left[\frac{n_1!}{(n_1+|l_1|)!}\frac{n_2!}{(n_2+|l_2|)!}\right]^{1/2}\sum_{\alpha=0}^{n_1}\frac{(-1)^\alpha}{\alpha!}\binom{n_1+|l_1|}{n_1-\alpha}\\&\times\sum_{\beta=0}^{n_2}\frac{(-1)^\beta}{\beta!}\binom{n_2+|l_2|}{n_2-\beta}(\alpha+\beta+(|l_1|+|l_2|-k)/2)!\sum_{p=0}^{\alpha+\beta+(|l_1|+|l_2|-k)/2}(-1)^p\\&\times\binom{\alpha+\beta+(|l_1|+|l_2|+k)/2}{k+p}\sum_{s=0}^{p}\frac{(-1)^s}{s!}\binom{p+k}{p-s}\frac{(R/a)^{2s}}{[1+(d/a)^2]^{s+p+k+1}},\end{aligned} \tag{4}$$

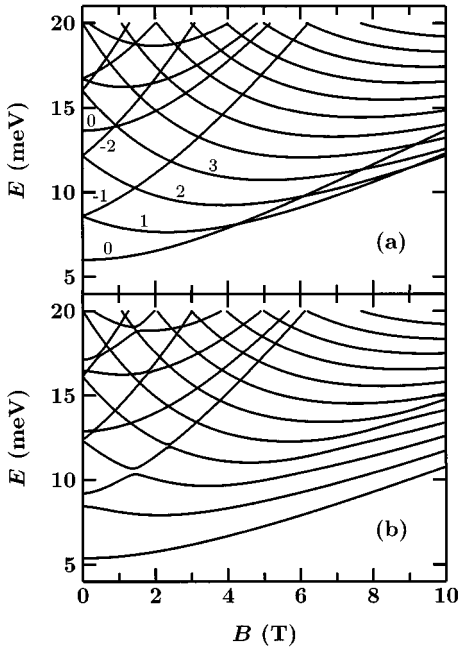

FIG. 1. Lowest single-electron energy levels vs magnetic field of a parabolic quantum dot containing a repulsive scatterer ($V_0=10$ meV, $d=5$ nm) located (a) at the center of the dot and (b) at 5 nm away from the center. In (a) some values of the angular momentum quantum number are indicated.

where $k=|l_1-l_2|$ and the position of the impurity $\mathbf{R}$ is represented in polar coordinates (R,Θ).

Intensities of the optical absorption are calculated within the electric-dipole approximation.[7] The normalized transition probability from the ground state Ψ_0 to an excited state Ψ_i is obtained from

$$\mathscr{A}_{0i}=|\langle\Psi_0|\mathbf{r}|\Psi_i\rangle|^2=\frac{1}{2}|\langle\Psi_0|r_+|\Psi_i\rangle|^2+\frac{1}{2}|\langle\Psi_0|r_-|\Psi_i\rangle|^2, \tag{5}$$

where $r_\pm$ are defined in the second quantized notation as[7]

$$r_\pm=\sum_{n_1,l_1,n_2,l_2}\int\varphi^*_{n_1l_1}(\mathbf{r})re^{\pm i\theta}\varphi_{n_2l_2}(\mathbf{r})d\mathbf{r}\;a^\dagger_{n_1l_1}a_{n_2l_2}. \tag{6}$$

The material parameters chosen for the numerical results presented below are appropriate for GaAs quantum dots, $\epsilon=13$, electron effective mass $m^*=0.067m_e$, and $\hbar\omega_0=4$ meV.

Some of the single-electron energy levels of a parabolic quantum dot with an impurity at the center are shown in Fig. 1(a). There are several features in the spectrum that distinguish it from that in an impurity-free parabolic dot.[1,3,8] First of all, the ground state has different angular momenta at different magnetic fields. Further, the impurity potential mixes energy levels that have the same angular momentum but different principal quantum number. The degeneracy at $B=0$ is partially lifted. Different Fock-Darwin bands[1] are clearly visible. The level spacings are also quite different from those in impurity-free parabolic quantum dots.

The energy levels of a parabolic quantum dot with an impurity that is near but not exactly at the center are shown in Fig. 1(b). Here the angular momentum is not a good quantum number and as one can see, all degeneracies at $B=0$ T are lifted. There is no abrupt change in the ground state as the magnetic field is changed. The anticrossings in the lowest Fock-Darwin band are clearly visible. There are several anticrossings also in the higher-energy levels. Comparing these results with those for an impurity-free parabolic dot one finds that the strength of the energy-level repulsion (anticrossing) depends strongly on the difference in the quantum numbers n and l of the appropriate states. The level repulsion is strongest for states that have the same value of n and that differ as little as possible in l.

Comparing Figs. 1(a) and 1(b) one can see that the level repulsion is strong for the levels in the lowest Fock-Darwin band. In Fig. 1(a) the $l=0$ state (i.e., the ground state at $B=0$ T) crosses some of the lowest-energy levels of the lowest band as the magnetic field is increased. But as soon as the circular symmetry is broken by moving the impurity away from the center [Fig. 1(b)] the states in the lowest Fock-Darwin band are mixed. This results in strong anticrossing such that only some hints of the original $l=0$ energy level can be seen at higher magnetic fields between energies 10 and 15 meV. The track of the original $l=0$ energy level becomes much clearer as it crosses the other levels with higher value of l, i.e., as the magnetic field is further increased.

A strong anticrossing effect can also be seen at $B=0$ T between states with $n=0$, $l=-1$ and $n=0$, $l=1$, i.e., $\Delta n=0$ and $\Delta l=2$. In Fig. 1(a) these two states are degenerate at $B=0$ T with energy eigenvalue about 8.6 meV. In Fig. 1(b) this degeneracy is clearly lifted due to the broken circular symmetry. Another strong anticrossing can be seen at $B=1.4$ T near the energy value of 10.5 meV. This anticrossing corresponds to the crossing of the energy levels with $n=0$, $l=-1$ and $n=0$, $l=2$ of Fig. 1(a). Here $\Delta l=3$ and the level repulsion is clearly weaker than the one between the states with $n=0$, $l=-1$ and $n=0$, $l=1$ where $\Delta l=2$. There is also an equally strong anticrossing at higher energy near $E=19$ meV and $B=1.4$ T. This anticrossing results from the level repulsion between states with $n=1$, $l=-1$ and $n=1$, $l=2$, i.e., here also $\Delta n=0$ and $\Delta l=3$. Although there seems to be many level crossings in Fig. 1(b) all these crossings are actually anticrossings. Because the strength of the level repulsion depends strongly on the difference in n and l the gap between many of the energy levels is too small to be seen in the Fig. 1(b). The fact that there are no crossings of the energy levels means also that there is no conserved quantity other than the energy. In that sense the system seems to be chaotic.

As the impurity is moved further away from the center of the dot, interactions between the states of the impurity-free dot first increase resulting in stronger anticrossing effects. But when the impurity is far enough its effects are reduced and the energy levels begin to resemble the levels of an impurity-free parabolic quantum dot.

The energy levels of a quantum dot containing two interacting electrons and the impurity at the center are shown in Fig. 2(a). Clearly, the spin singlet-triplet transition is moved from about 2.5 T (impurity-free case) to about 1.5 T due to the presence of the scatterer. Similar results for systems where the impurity is moved away from the center are shown

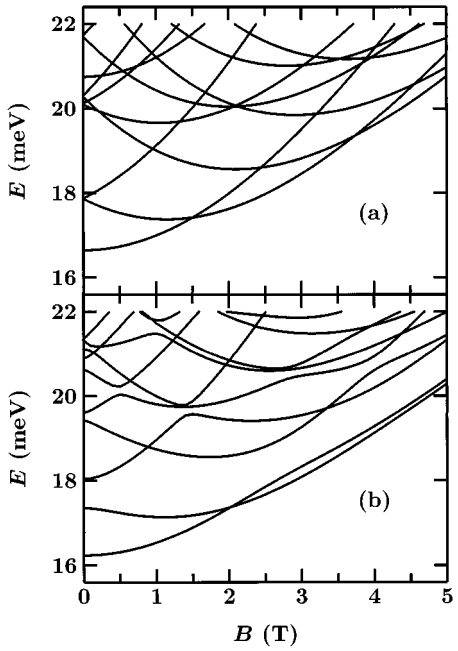

FIG. 2. Lowest-energy levels of a two-electron parabolic quantum dot containing a repulsive scatterer ($V_0=10$ meV and $d=5$ nm) located (a) at the center of the dot and (b) at 5 nm away from the center.

in Fig. 2(b). As expected, there is no degeneracy at $B=0$ T. Clear energy level repulsion can also be seen in this case.

We have made a detailed analysis of how the energy levels shown in Fig. 2(a) are changed as the impurity is moved away from the center of the dot. Just like the single-electron energy levels (Fig. 1) here also we find angular momentum selection rules that govern the strength of the level repulsion. If the angular momentum of a pair of crossing energy levels of Fig. 2(a) differs by two there is a large anticrossing of the corresponding levels in Fig. 2(b). If the difference is some other even number then the anticrossing is weaker but still not insignificant. However, if the difference of the angular momentum quantum numbers is an odd integer then the level repulsion is almost negligible. Since we are dealing here with two mutually interacting electrons with opposite spins it is evident that the change from the one-electron case in the rules governing the strength of the level repulsion is due to the Coulomb force.

We have done similar types of calculations for three- and four-electron dots. These calculations support, for electron numbers higher than one, a simple rule that if there is an even (odd) number of electrons, the level repulsion is strong for states that correspond to the states in a corresponding circularly symmetric system (i.e., impurity is at the dot center) whose angular momentums differ by an even (odd) number.

Figure 3 shows optical absorption of a quantum dot containing one impurity that is near but not at the center of the dot and one, two, and three electrons. Preliminary results for one and two electrons have already been published.[9] The point here is that any increase of the number of electrons will result in a decrease of the effect of the impurity on the optical absorption. In the one-electron dot the degeneracy of the absorption modes at $B=0$ T is clearly lifted. But as the number of electrons is increased the level repulsion decreases substantially. Also the clear structures seen in the one- and two-electron results have almost all disappeared in the three-electron case; the optical absorption intensity is more or less scattered around the original modes of an impurity-free quantum dot.

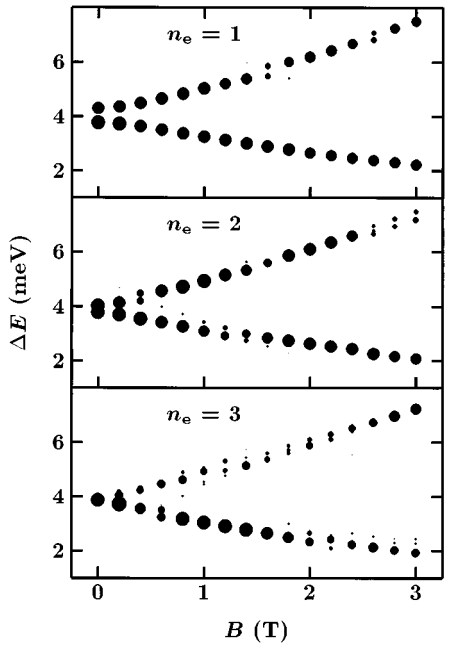

FIG. 3. Dipole-allowed optical absorption energies and intensities of a parabolic quantum dot containing a repulsive scatterer ($V_0=4$ meV and $d=5$ nm) located 5 nm away from the center of the dot. Areas of the filled circles are proportional to the calculated absorption intensities. The number of electrons in the dot is indicated inside the figures.

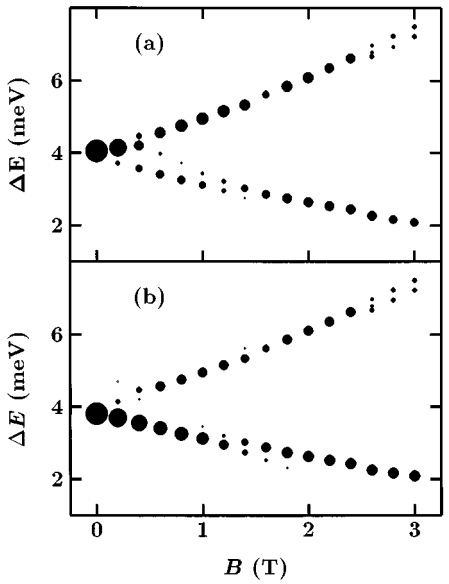

FIG. 4. Dipole-allowed optical absorption energies and intensities of a parabolic two-electron quantum dot containing a repulsive scatterer ($V_0=4$ meV and $d=5$ nm) located 5 nm away from the center of the dot at x axis. The absorbed electromagnetic radiation is linearly polarized with the electric field pointing (a) along the x axis and (b) along the y axis.

Figure 4 shows optical absorption of a two-electron quantum dot containing one impurity that is near but not exactly at the center of the dot. The absorbed light is now linearly polarized. The main result here is that the polarization affects the absorption only at low magnetic fields. If the electric field of the electromagnetic radiation points along the axis that goes through both the center of the dot and the center of the impurity, i.e., x axis, the absorption is strongest for the so-called bulk mode (the upper mode) at low magnetic fields [Fig. 4(a)]. If the absorbed radiation is polarized perpendicular to that axis, i.e., along y axis, the absorption is strongest for the edge mode (the lower mode) at low magnetic fields [Fig. 4(b)]. As the magnetic field is increased the difference on the absorption intensity between these two polarization directions quite rapidly disappears. One explanation to this effect could be that the electron density near the impurity decreases as the magnetic field is increased. This is because the electron density moves away from the center towards the edges of the dot as the magnetic field is increased.

Finally, in Fig. 5 we show optical absorption of a quantum dot containing five impurities and one, two, and three electrons. Clear similarities with one-impurity results (Fig. 3) can be seen here. The main difference is that the degeneracy at $B=0$ T is not so strongly lifted, i.e., the system is effectively more circularly symmetric than in the one impurity case. Here also the increase of the number of electrons decreases the effects of the impurities.

In closing, we have analyzed the effect of repulsive scatterers in a quantum dot subjected to a perpendicular magnetic field. Our study reveals the angular momentum selection rules that govern the level repulsion when the scatterer is moved away from the center of the dot. The optical absorption spectrum is also calculated in this case. We find that depending upon the polarization of the radiation, the absorption of the bulk or edge modes are dominant. Further work on optical, transport, and capacitance spectroscopic measurements[4] are needed to observe the features explored here.

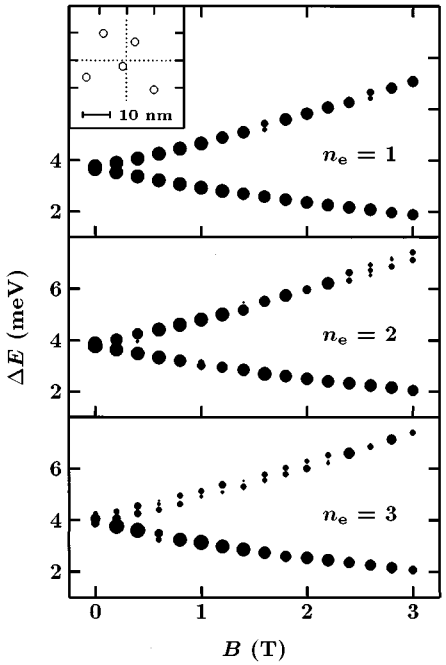

FIG. 5. Dipole-allowed optical absorption energies and intensities of a parabolic quantum dot containing five repulsive scatterers. The locations of the scatterers, which are denoted as open circles and with parameters $V_0=2$ meV and $d=5$ nm, are shown in the inset. Areas of the filled circles are proportional to the calculated absorption intensities. The number of electrons in the dot is also indicated.

[1] For a review see, T. Chakraborty, Comments Condens. Matter Phys. **16**, 35 (1992).

[2] *Proceedings of the Workshop on Novel Physics in Low-Dimensional Electron Systems, Madras, India, 1995*, edited by T. Chakraborty [Physica B **212**, 201 (1995)].

[3] P. A. Maksym and T. Chakraborty, Phys. Rev. Lett. **65**, 108 (1990); Phys. Rev. B **45**, 1947 (1992); P. A. Maksym, Physica B **184**, 385 (1993); F. Bolton, Phys. Rev. Lett. **73**, 158 (1994); V. Halonen, T. Chakraborty, and P. Pietiläinen, Phys. Rev. B **45**, 5980 (1992); A. V. Madhav and T. Chakraborty, *ibid.* **49**, 8163 (1994); V. Halonen, Solid State Commun. **92**, 703 (1994).

[4] R. C. Ashoori *et al.*, Phys. Rev. Lett. **71**, 613 (1993); P. L. McEuen *et al.*, *ibid.* **66**, 1926 (1991); Phys. Rev. B **45**, 1141 (1992); **45**, 11 419 (1992); A. Zrenner *et al.*, Phys. Rev. Lett. **72**, 3382 (1994); Ch. Sikorski and U. Merkt, *ibid.* **62**, 2164 (1989); M. A. Reed *et al.*, *ibid.* **60**, 535 (1988).

[5] C. Weisbuch and B. Vinter, *Quantum Semiconductor Structures* (Academic, New York, 1991); *Nanostructured Systems*, edited by M. A. Reed (Academic, San Diego, 1992); T. J. Thornton, Rep. Prog. Phys. **58**, 311 (1995).

[6] A. S. Sachrajda *et al.*, Phys. Rev. B **50**, 10 856 (1994).

[7] T. Chakraborty, V. Halonen, and P. Pietiläinen, Phys. Rev. B **43**, 14 289 (1991); R. Ugajin, *ibid.* **51**, 10 714 (1995); **51**, 11 136 (1995).

[8] V. Fock, Z. Phys. **47**, 446 (1928); C. G. Darwin, Proc. Cambridge Philos. Soc. **27**, 86 (1930).

[9] P. Pietiläinen V. Halonen, and T. Chakraborty, in *Proceedings of the Workshop on Novel Physics in Low-Dimensional Electron Systems* (Ref. 2).